Aerostatic and buffeting response characteristics of catwalk in a long-span suspension bridge

Yongle Li[*1], Dongxu Wang[1], Chupeng Wu[1] and Xinzhong Chen[2]

[1]*Department of Bridge Engineering, Southwest Jiaotong University, Chengdu, Sichuan 610031, P. R. China*
[2]*Wind Science and Engineering Research Center, Department of Civil and Environmental Engineering, Texas Tech University, Lubbock, Texas 79409-1023, USA*

Abstract. This study presents a comprehensive investigation of the aerostatic and buffeting response characteristics of a suspension bridge catwalk. The three-dimensional aerostatic response analysis was carried out taking into account the geometric nonlinearity and nonlinear dependence of wind loads on the angle of attack. The buffeting response analysis was performed in the time domain. The aerostatic and buffeting responses of the catwalk show strong coupling of vertical and lateral vibrations. The lateral displacement is the main component of the wind-induced static and buffeting response of the catwalk.

Keywords: catwalk; aerostatic response; buffeting response; suspension bridge

1. Introduction

A catwalk, arranged under the main cable, is a false-work for the erection of the main cable of a suspension bridge. The construction of a main cable requires erection high above the ground, which results in strong wind acting on the catwalk. On the other hand, the characteristics of a slender long-span structure makes a catwalk highly sensitive to the action of wind loading. Under the action of strong wind loading, a catwalk may develop extensive static deformation and even become statically unstable at very high wind speed. In addition, wind fluctuations may cause significant buffeting acceleration response that affects the safety and comfort of workers and impacts on the quality and efficiency of the construction process. Better understanding and assessment of the performance of catwalk under strong wind is therefore important for the construction of long-span suspension bridges.

Since the Tacoma Narrows Bridge failure of 1940, numerous researchers have made significant contributions to the characterization and modeling of wind loads on bridges using wind-tunnel testing, and on the evaluation of the performance of long-span bridges under turbulent wind actions (Davenport 1962, Scanlan 1978, Xu and Sun 1998, Chen and Kareem 2001). Multi-mode coupled analysis frameworks in both time and frequency domains have been developed for bridge flutter and buffeting (Jain *et al.* 1996, Chen *et al.* 2000). Analysis frameworks are also under development to take into account the influence of non-linear structural

---

*Corresponding author, Professor, E-mail: lele@swjtu.edu.cn

and aerodynamic characteristics. Static divergence, that is non-oscillatory aero-elastic instability, has also attracted considerable attention for longer spans. In the case of catwalks, flutter instability is generally not observed due to the low solidity ratios of the bottom and side mesh construction. However, static deformation and random buffeting response have been of concern for the design of catwalks (Larsen 1997, Shinichi 1997)

The static stability of the catwalk of a suspension bridge with a main span of 960 m was addressed by Zheng *et al.* (2007), using a nonlinear finite element (FE) model and the mean (static) aerodynamic force coefficients determined through section model test in wind tunnel. The prediction was also compared with the result from a full aero-elastic model tunnel test. Kwon *et al.* (2012) studied the influence of Reynolds number, the existence of a main cable and the ventilation rate of the meshwork on the mean aerodynamic force coefficients of a catwalk. Static and buffeting analysis were also carried out to study static and dynamic response of the catwalk, and to evaluate the performance of different design configurations and vibration mitigation measures.

Storm ropes were previously installed to improve the wind-resistant performance of catwalks. In recent years, in order to accelerate the construction process and reduce the cost, suspension bridge catwalks have tended to adopt gantries rather than storm ropes, which make the catwalks even more flexible and thus more sensitive to wind loading. This study focused on the static and buffeting response of a catwalk with gantries. A three-dimensional aerostatic response analysis was carried out taking into account the geometric nonlinearity and nonlinear dependence of wind loads on angle of attack. The buffeting response analysis was performed in the time domain. The mechanism of unique coupling between vertical and lateral vibrations is discussed in detail.

2. Finite element model of the catwalk system

2.1 Finite element model and modal analysis of catwalk system

The catwalk of a suspension bridge with a main span of 820 m is considered. The span configuration is 192 m (north span) + 820 m (mid span) + 176 m (south span), with simply supported steel box girder. The two parallel main cables at main span center are 75.3 m above the bridge deck. The catwalk is a separate structure and is not assembled with wind-resistant cables. The line shape of the catwalk is parallel to the centerline of the main cable with a separation distance of 1.5 m. There are seven cross bridges between two catwalks, i.e., one in each side span, five in main span, with a space of 135 m between adjacent cross bridges, in order to increase the transversal stiffness. The layout and the elevation of the catwalks are shown in Figs. 1 and 2. Each catwalk consists of load-bearing ropes, gantry ropes, handrail ropes, meshwork, gantries, cross bridges and anchor system. The meshwork is comprised of two layers of steel wire mesh and anti-skid battens. A local view of the catwalks is shown in Fig. 3.

A three-dimensional finite element model was established using software ANSYS, with a special finite elements. The rigidity of the non-load-bearing structure (the steel wire gauze, the manrope, the railing rope, the hand banisters, and the lateral protective screening) was ignored, but the weight was included in the modeling. The head-rope of the catwalk was modeled using a cable element 'Link10', in which the influence of initial axial force on the geometric stiffness is considered. A cable element can only support tensile stress but not compressive stress. The cross beam, the cross bridge and the bridge tower were modeled by element 'Beam44'. The finite element model used is shown in Figs. 4 and 5.
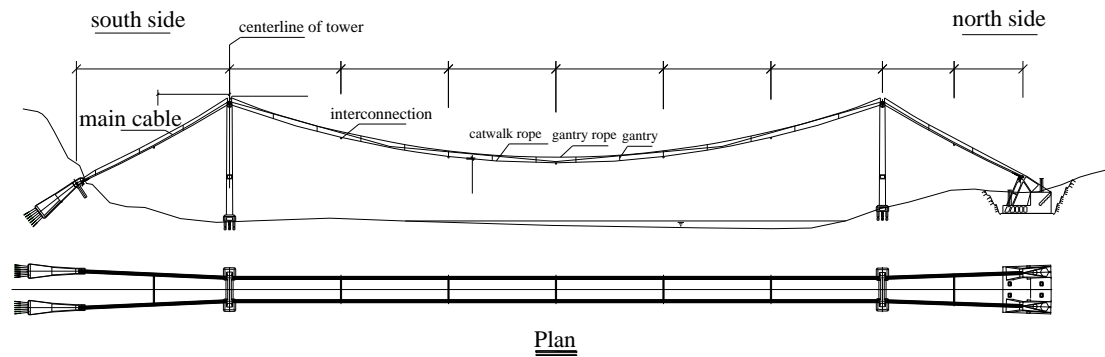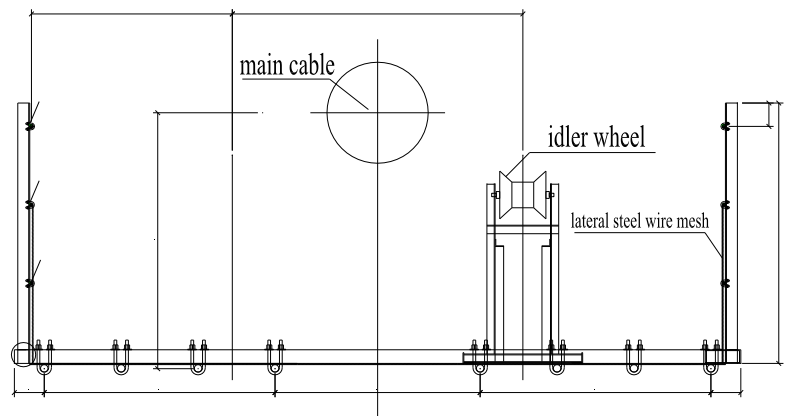
Fig. 1 Lay-out of the catwalks

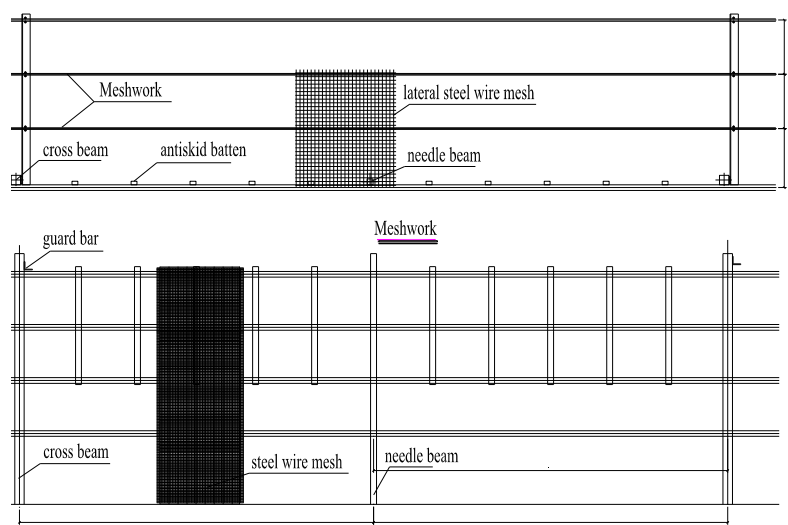Fig. 2 Elevation view of the catwalks
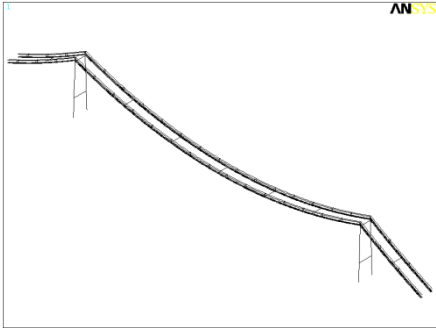

Fig. 3 Local view of the catwalks
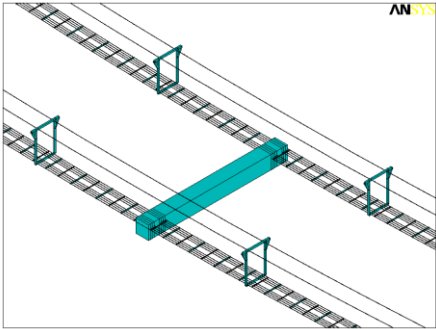
Fig. 4 Full finite element model

Fig. 5 Local finite element model

The catwalk is a typical cable-truss structure. Its modal analysis was carried out considering pre-stress effects. The static response analysis was first conducted, and then modal analysis was carried out around the statically deformed equilibrium. The natural frequencies of the first 10 modes under zero wind speed are listed in Table 1, and the mode shapes of the first symmetric lateral, vertical and torsional modes are also given in Figs. 6-8.
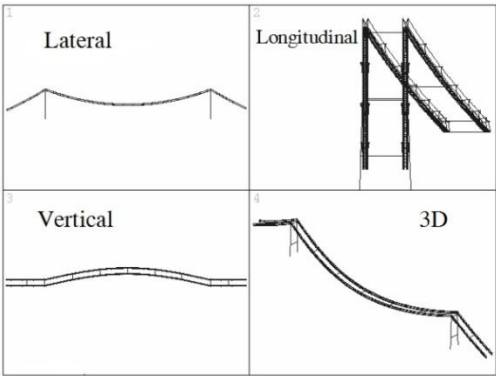

Fig. 6 First lateral bending mode

Table 1 Natural modal frequencies of the catwalk (Hertz)

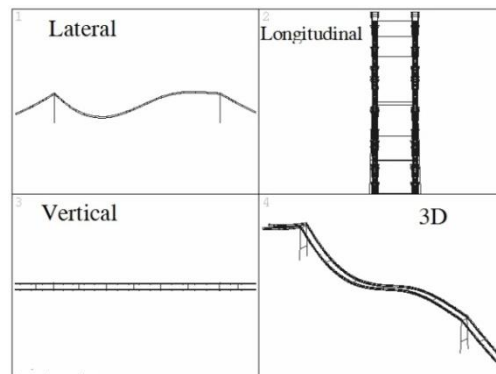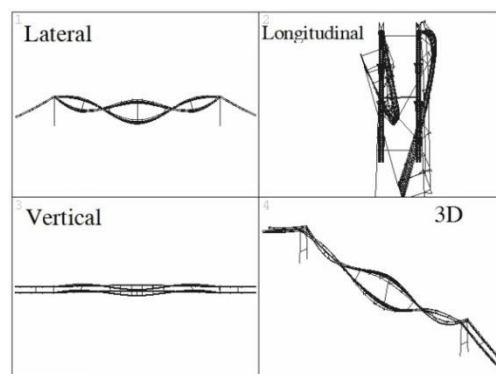| Mode number	Characteristics of mode	Natural frequency
1	1st symmetric lateral bending	0.0638
2	1st anti-symmetric lateral bending	0.1231
3	1st anti-symmetric lateral bending + 1st anti-symmetric vertical bending +1st anti-symmetric torsion	0.1256
4	1st anti-symmetric lateral bending + 1st anti-symmetric vertical bending +1st anti-symmetric torsion	0.1293
5	1st symmetric vertical bending	0.1741
6	1st symmetric torsion	0.1827
7	2nd symmetric lateral bending	0.1895
8	1st symmetric vertical bending of side-span	0.2228
9	2nd anti-symmetric vertical bending	0.2464
10	2nd anti-symmetric lateral bending +2nd anti-symmetric vertical bending	0.2504

Fig. 7 First vertical bending mode

Fig. 8 First torsional mode

2.2 Wind tunnel test with section model of the catwalk

The section model wind tunnel test was carried out to determine the mean (static) aerodynamic force coefficients. The reduced scale of the model was 1/6. The model had a length of 2.10 m, a width of 0.708 m and a height of 0.254 m, as shown in Fig. 9. As the distance between two catwalks is far larger than the width of catwalk, and the catwalk is composed of some steel wire meshes through which air can pass freely, the aerodynamic interaction between two catwalks is considered to be very weak. The mean force coefficients were obtained from a wind-tunnel test of only one catwalk, and were applied to the aerostatic analysis of the catwalk system. The wind-tunnel measurements were performed in smooth flow. To check the potential influence of Reynolds number, the test was repeated at three different wind speeds, i.e., 10, 15 and 20 m/s. The range of attack angle was $-12^0 \sim +12^0$. The drag, lift and pitching moment coefficients are shown in Fig. 10. The results from different wind speeds are identical, indicating that the influence of Reynolds number is negligible.
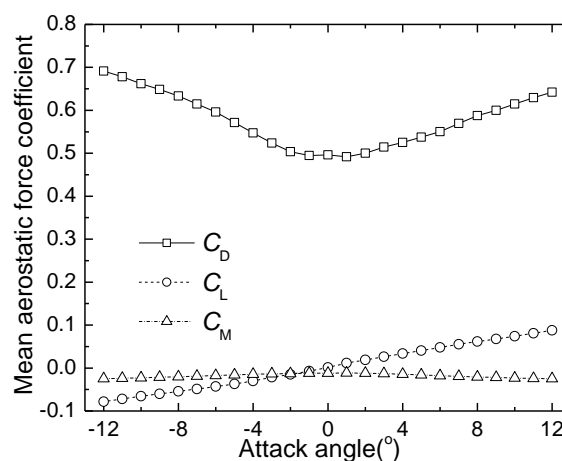

Fig. 9 Section model of catwalk

Fig. 10 Mean aerodynamic force coefficients from a wind-tunnel test

3. Analysis of static response and aerostatic stability

3.1 Analysis with three-dimensional non-linearity

The static response of the catwalk can be calculated by solving the following non-linear equation (Thai and Kim 2011), where the geometric non-linearity of the catwalk and the non-linear dependence of the mean wind force on angle of attack are included

$$\left[K_e(\{Y\}) + K_g^{G+W}(\{Y\})\right]\{Y\} = \{F(\alpha)\}$$

$[K_e]$ and $[K_g]$ represent the linear and geometric stiffness matrices of structure; $\{Y\}$ is the displacement vector of structure; α is effective attack angle; $\{F\}$ represents the external wind force vector including the effect of drag force, lift force and pitching moment; and G and W represent the gravity and wind load. In the whole analysis, the axial stress of catwalk is in linear and elastic range of the material. Thus the non-linearity of material is ignored.

The torsional displacement of the catwalk increases with the increasing wind speed, which leads to a change in mean aerodynamic forces, as the force coefficients vary with the angle of attack. Thus, there exists non-linear relationship between the deformation of structure and the static wind load. As the non-linearity of the geometric stiffness depends on both the displacement and the angle of catwalk, it is necessary to extract the torsional displacement from the displacement matrix and correct the attack angle in order to execute iteration to obtain an equilibrium state. This study adopted the incremental method and internal-external iteration method to analyze the static response and aerostatic stability (Cheng *et al*. 2002). Considering the effects of geometric non-linearity and the aerostatic load non-linearity, the aerostatic load increment and double iterations are combined to analyze the aerostatic stability of the catwalk (Li *et al*. 2009).   The wind speed was increased step by step in order to trace the development of the deformation with wind speed. At a given wind speed, the internal iteration method was applied to carry out the analysis of geometric non-linearity while the external iteration method was applied to find out the equilibrium position of structure. The analysis procedure is as follows:

a) According to the torsion displacement of structure at previous wind speed $\{\theta\}_{n-1}$,calculate effective angle of attack α and the wind load under the given wind speed;

b) Determine the displacement vector by applying Newton-Raphson Method (Shinichi 1997) to account for the geometric nonlinearity;

c) Extract the torsional displacement $\{\theta\}_n$ from the displacement vector and calculate the increment of torsion angle $\{\Delta\theta\}_n = \{\theta\}_n - \{\theta\}_{n-1}$;

d) Verify whether the maximum torsional increment satisfies the given convergence criterion (0.002 degree is adopted in this study);

e) If the criterion is not satisfied, repeat the calculation of steps (a) to (d) with $\{\theta\}_n = \{\theta\}_n + \varphi\{\theta\}_n$,where φ is relaxation factor and 0.5 is used in this study;

f) If the criterion is satisfied, stop the calculation for the given wind speed.

3.2 Aerostatic response and stability of the catwalk

The static response and stability analysis were conducted at three initial angles of attack, i.e., $\alpha = -3^0, 0^0 \text{ and } +3^0$ at wind speeds up to 90 m/s. The lateral, vertical and torsion displacements at 0 degree angle of attack are shown in Figs.11 to 13. The maximum lateral and vertical displacements

are both located at the center of main span, while the maximum torsion angle is observed at the center of short span, between the cross bridges near bridge tower.

It is noted that the spanwise variation of torsion displacement is different from previous studies (Li *et al.* 2013), which is attributed to the existence of gantries. In the case of catwalk without gantry addressed in previous studies, the torsional stiffness is mainly controlled by the cross bridges. The maximum torsional displacement is located in the middle of two cross bridges in the center of main span. The catwalk of this study has both gantries and cross bridges that enhance the stiffness and restrict the torsional displacement. Thus, the torsional displacements at the positions of gantry and cross bridge are small due to the restriction of these components as shown in Fig. 13.

Fig. 11 Lateral displacement under different wind speed
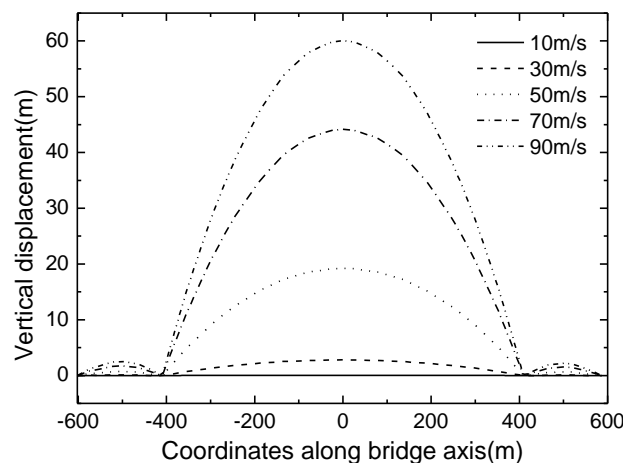

Fig. 12 Vertical displacement under different wind speed

The spanwise variation of torsional displacement shows characteristics of local modes rather than a global trend (the first torsional mode) in Fig. 8. The distribution of torsional displacement is not mainly determined by the first torsional mode shape, but is a combination of the first several modes of lateral, and vertical and torsional vibrations. In addition, the first torsional mode (the sixth vibration mode of catwalk) makes a relatively lower contribution to the main vibration pattern of the catwalk. The distribution of torsional angle is the direct and objective response of the structure under static wind loading, which is in accord with the structural mechanical property of the catwalk. In order to illustrate the variation character of torsional displacement along bridge axis, the nominal torsional stiffness at different spanwise locations was calculated; this is defined as the torque needed to generate a unit torsional displacement at a point of catwalk. The distribution of nominal torsional stiffness is shown in Fig. 14. The nominal torsional stiffness is large in the position of gantries and cross bridges and has a small value at the center of each span.
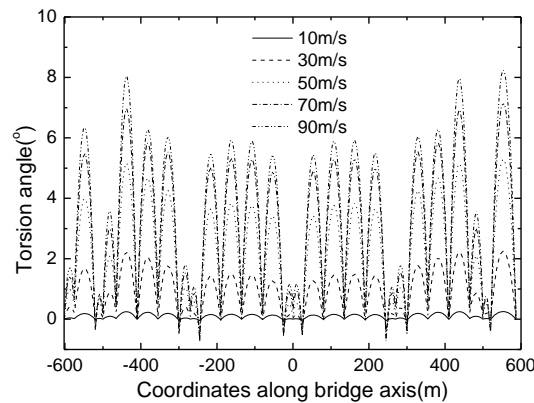

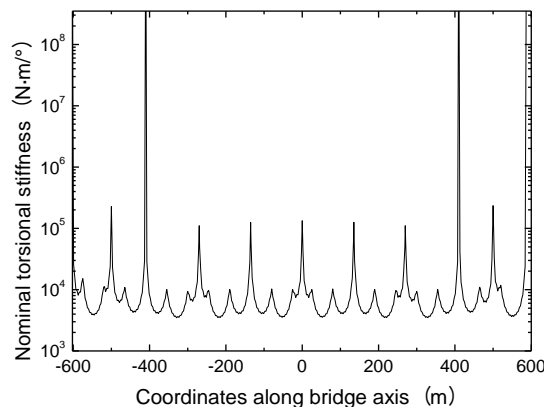Fig. 13 Torsion angle under different wind speed

Fig. 14 Nominal torsional stiffness along bridge axis

Figs. 15-17 display the maximum displacements as functions of wind speed. Figs. 18-20 show the drag force, lift force and pitching-moment per unit length in the positions of maximum displacement. As expected, the catwalk displacements increase with increasing wind speed. From the increasing rate of displacements, it is clear that static divergence does not occur for wind speed up to 90 m/s.

As the static wind load is proportional to the square of wind speed, the predicted static displacements should increase with increasing wind speed, following a quadratic parabola if structural and aerostatic nonlinearities are not included. It is observed from Fig. 15 that the increasing rate of lateral displacement with wind speed reduces at higher wind speeds. The increase of static drag force coefficient with increasing angle of attack should have made the lateral displacement more sensitive to the increase in wind speed. Clearly, this reduced sensitivity of lateral displacement on wind speed is caused by the geometric non-linearity of the lateral stiffness that increases with increasing lateral displacement. Fig. 21 displays the variation of the first lateral, vertical and torsional frequencies with increasing wind speed. It is clearly observed that the geometric stiffness in three directions has an obvious increment at high wind speeds. The geometric stiffness increases due to large deformation of structure, and will restrict further deformation, demonstrating the convergent trend of displacement at high wind speeds.
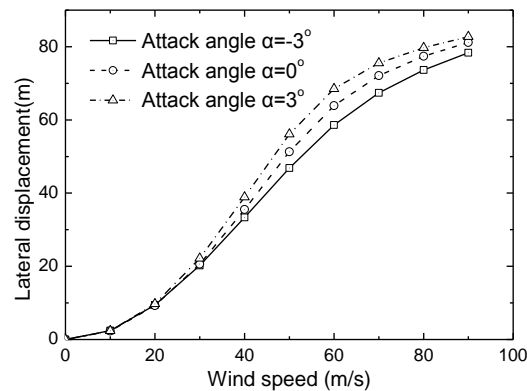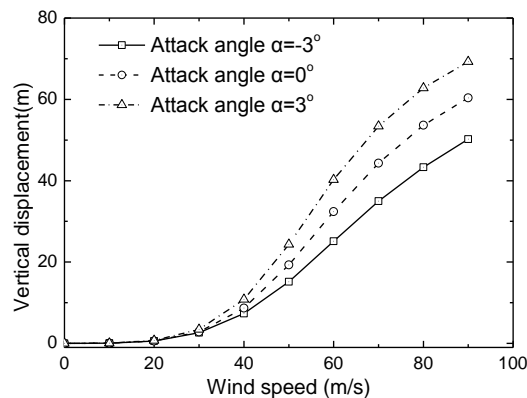

Fig. 15 Maximum lateral displacement

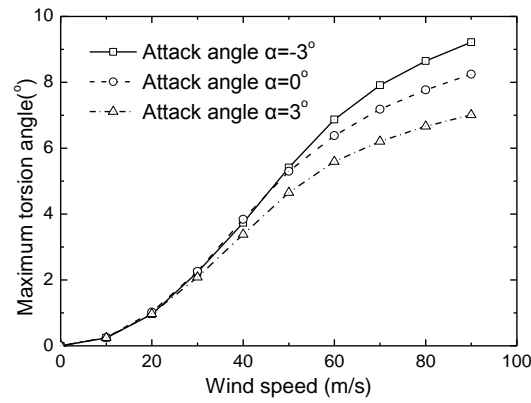Fig. 16 Maximum vertical displacement
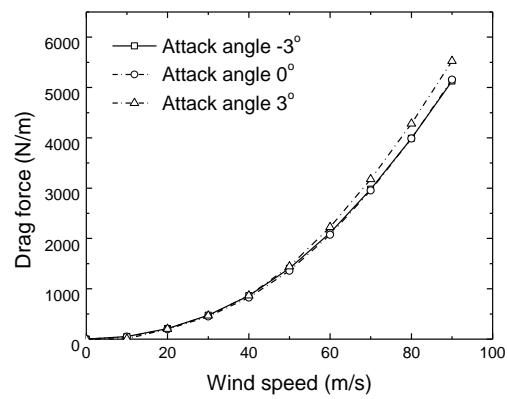
Fig. 17 Maximum torsion angle
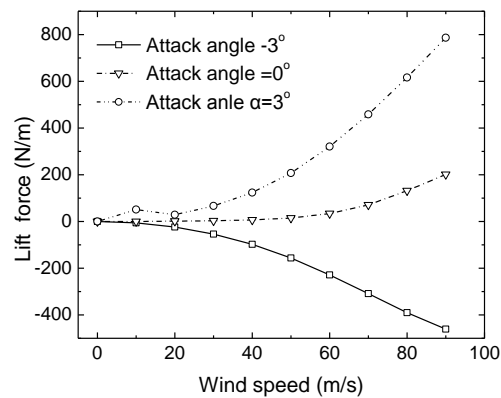
Fig. 18 Drag force in the center of main span

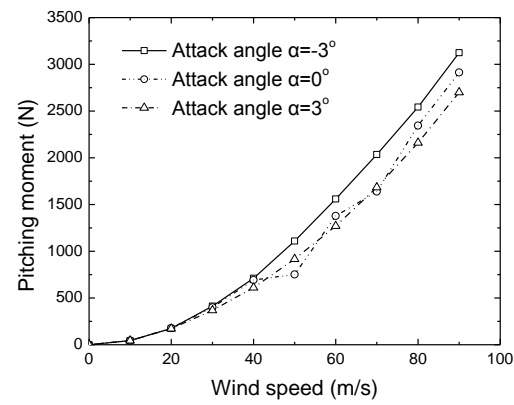Fig. 19 Lift force in the center of main span

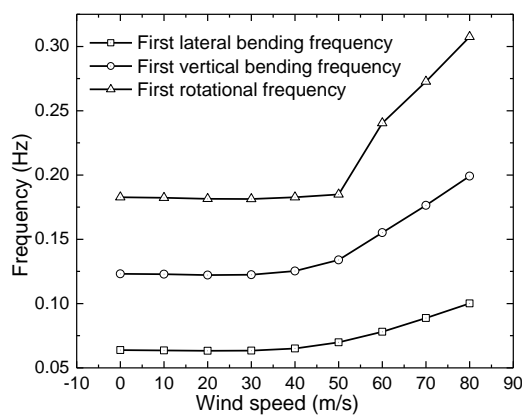Fig. 20 Pitching moment in the node of maximum torsion angle

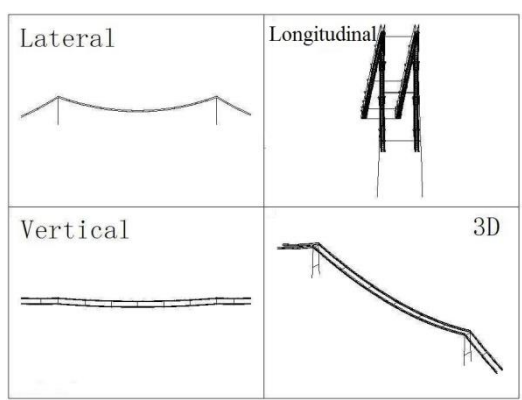Fig. 21 Modal frequency under different wind speed

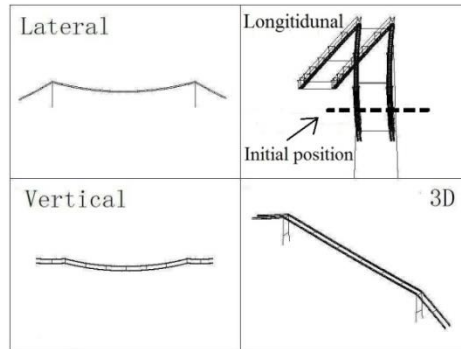Fig. 22 Static deformation under wind of 25.7 m/s

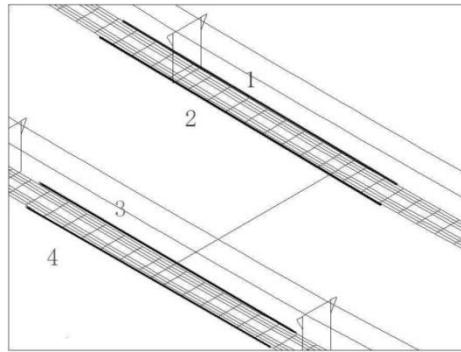Fig. 23 Static deformation under wind of 50 m/s

Fig. 24 Local view of 4 cables

It is also noted that the deformations of catwalk at different initial angle of attack are consistent with the dependence of force coefficients on the angle of attack. The lateral and vertical deformations under positive attack angle are larger than those for negative attack angles, while the torsional displacement is smaller under positive angle of attack. The lift force is much smaller than the drag force as shown in Figs. 18 and 19, but the vertical displacement under high wind speeds is almost the same as the lateral displacement. Figs. 22 and 23 show the static deformation of catwalk under wind speed of 25.7 and 50 m/s, respectively. It is easily observed that lateral motion would induce vertical displacement, which is more evident with high wind speeds. It is a result of coupling between lateral and vertical motions.

Fig. 24 shows a local view of four cables of catwalk, in which cable 1 is located in the windward side. Fig. 25 displays the vertical displacements of these four cables under wind speed of 25.7 m/s. The vertical displacement of the windward cable and that of the leeward cable are almost the same, which illustrates that the vertical displacement is not due to the coupling of lateral displacement and global torsional displacement, but due to the coupling between lateral and global vertical motions. This coupling mechanism is a result of the high flexibility of catwalk, which is very different from the suspension bridge deck, for which the coupling of lateral and vertical motions is very weak while the coupling of lateral and torsional motions is very significant.
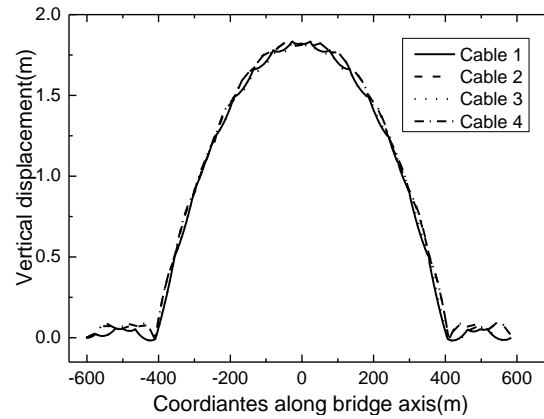
Fig. 25 Vertical displacement of 4 cables

4. Buffeting analysis of catwalk

4.1 Buffeting force model and simulation of wind field

For the typical cable-truss structure of catwalk and the geometric non-linearity, a time-domain method for the buffeting analysis of catwalk under natural wind was adopted (Kimura and Tanaka 1992, Ding and Lee 2000). The shape of catwalk in an upright plane is curved. The fluctuating wind velocity field was simulated by the spectral representation method with the Cholesky explicit decomposition of cross-spectral density matrix (Cao *et al*. 2000). In order to facilitate the calculation, it is assumed that fluctuating wind field characteristics changes along the direction of span but will not change along the direction of height. It is generally assumed that the wind fluctuations in three orthogonal directions are mutually uncorrelated. The overall three-dimensional (i.e., three components of natural wind) wind velocity field can be simplified into many one-dimensional wind velocity fields. The FFT (Fast Fourier Transform) technique was adopted to further improve the computational efficiency (Li *et al*. 2004). The random wind field in terms of lateral and vertical components was generated at 199 locations arranged at the 1/3 height of catwalk with a separation of six metres. A Kaimal turbulence spectrum, as required by the China wind-resistant design regulations (Ministry of Transport 2004), was adopted as the target spectrum for the lateral and vertical directions. A coherence function with a decay factor of 7, (Davenport 1962b), was used. The spectrum frequency ranged from 0.1 to 2 Hz, and the total time of simulation was 1280 s with a time-step of 0.25 s.

Self-excited forces were not considered, as their resulting aerodynamic damping at relative low wind speed can be considered to be negligible. The neglect of positive aerodynamic damping also leads to a conservative estimation of buffeting response. The buffeting forces are given by the following quasi-steady formulae in terms of wind fluctuations (Davenport 1962b)

$$D_{\mathrm{b}}(t) = \frac{1}{2}\rho U^2 H \left[2C_{\mathrm{D}} \frac{u(t)}{U} + C'_{\mathrm{D}} \frac{w(t)}{U} \right]$$

$$L_b(t) = \frac{1}{2}\rho U^2 B \left[2C_L \frac{u(t)}{U} + (C'_L + \frac{H}{B} C_D) \frac{w(t)}{U} \right]$$

$$M_b(t) = \frac{1}{2}\rho U^2 B^2 \left[2C_M \frac{u(t)}{U} + C'_M \frac{w(t)}{U} \right]$$

where ρ is air density; C_D, C_L, C_M are drag, lift and pitching moment coefficients; C_D', C_L', C_M' are their derivatives with respect to the angle of attack; U is mean wind speed; u and w are fluctuating wind speed in lateral and vertical directions.

4.2 Time domain analysis of catwalk buffeting

The time histories of buffeting forces can be readily calculated from the simulated fluctuating wind field. It was combined with the ANSYS transient dynamic analysis module to determine the time history of buffeting response. Figs. 26 to 28 show the root-mean-square (r.m.s.) values of buffeting displacements along with static displacements in lateral, vertical and torsional directions at the design mean wind speed of 25.7 m/s. The r.m.s. buffeting displacement in the main span is larger than that in side span. The maximum ratio of r.m.s. lateral displacement to static displacement is located at the center of main span with a value of 40 percent. The lateral buffeting response of catwalk under fluctuating wind is obvious. The r.m.s. lateral displacement of catwalk is much larger than the r.m.s. vertical displacement. As shown in Fig. 28, the r.m.s. torsional displacement has a very different spanwise variation from the static displacement. The disparity is reflected in two respects: local variance of the r.m.s. torsional displacement and small numerical values of static wind displacement. At the positions 0m, -270 m and 270 m on the catwalk marked in Fig. 28, a cross bridge is arranged in the middle of two gantries as shown in Fig. 5. The existence of cross bridge and gantry restricts the torsional displacement, and its r.m.s. value should be lower than the neighboring values.
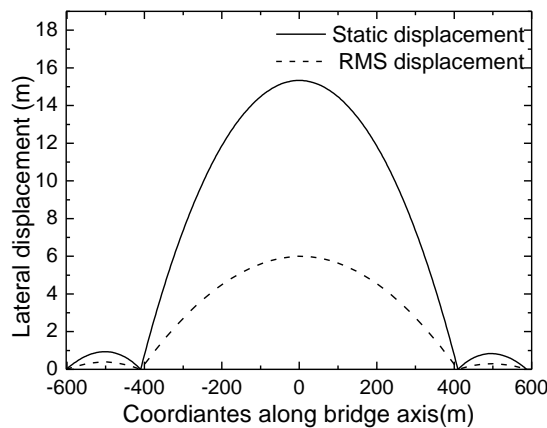

Fig. 26 Lateral displacement under calm wind and mean square root
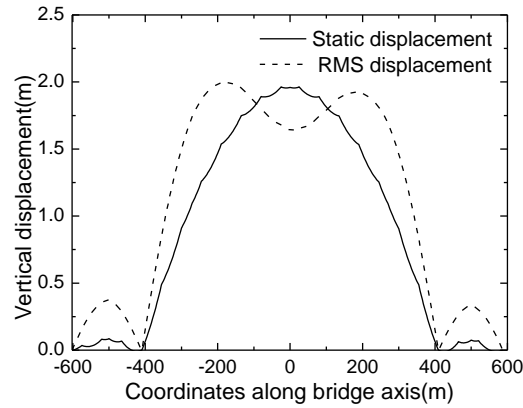
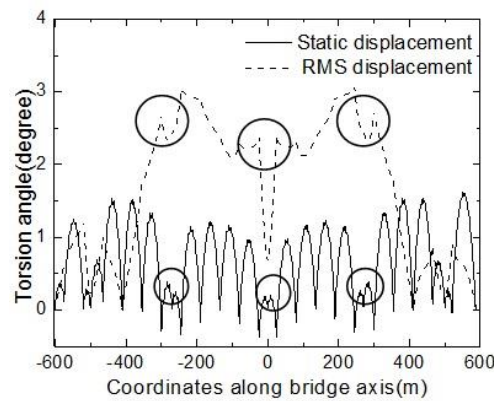Fig. 27 Vertical displacement under calm wind and mean square root

Fig. 28 Torsion angle under calm wind and root mean square

Regarding the small numerical values of static wind displacement, Fig. 22 shows the static deformation of catwalk under a design wind speed of 25.7 m/s. It is easily observed that lateral displacement would induce vertical motion but not torsional deformation, which shows the small torsional displacement under static wind.

The large r.m.s. torsional displacement is not only induced by pitching moment, but also by drag and lift buffeting forces. Drag and lift force even play the major role in the generation of torsional displacement and its r.m.s. value. Fig. 29 shows the r.m.s. torsional displacement calculated by using four different force models: 1) Original model where lift, drag and pitching moment on catwalk are included; 2) lift force model in which only lift force is considered; 3) drag force model in which only drag force is considered; and 4) Pitching moment in which only pitching moment is considered. It is observed that the span-wise variation of the r.m.s. values in the lift force model shows strong similarity to that in the original model. Howver, the r.m.s. value of the pitching moment is much smaller. The lift force is the dominant force component that causes the r.m.s. torsional displacement.
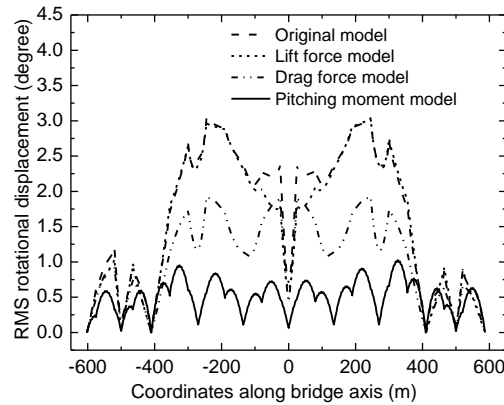
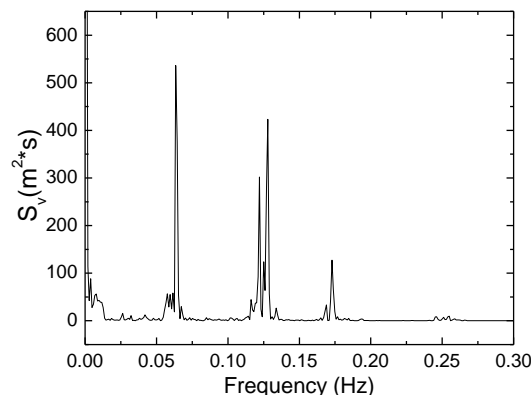Fig. 29 Torsion angle for four different models

Fig. 30 Power spectrum of vertical displacement time-procedures at 3/8 span

The coupling of vertical and torsional buffeting responses can also be identified from the response power spectra. The power spectra of vertical and torsional displacements at 3/8 span are shown in Figs. 30 and 31. It can be observed that both have a predominant frequency of 0.1279 Hz, which corresponds to the fourth mode with coupled lateral, vertical and torsional deformation as shown in Fig. 33 and Table 2. In Fig. 30, the first and the second peaks correspond to the symmetric and the anti-symmetric lateral bending frequencies while the third peak corresponds to the vertical bending frequency, which indicates that the lateral bending mode has greater contribution to vertical response. The static deformation of catwalk in Fig. 22 shows that lateral displacement induces vertical motion, but not torsional deformation. However, the second modal shape of catwalk in a wind speed of 25.7 m/s in Fig. 32 shows obvious torsion. The coupling effect of vertical displacement and torsional displacement is obvious under buffeting loading, while this coupling effect is not obvious in the aerostatic response.

The amplitude spectra of lateral and vertical displacements at mid span and 1/4 span are shown in Fig. 34 to Fig. 37. It can be observed that the lateral displacement is dominated by the first symmetric lateral mode with a frequency of 0.0641 Hz. This modal response also has a significant

contribution to the vertical displacement, especially at the mid span, as the first lateral bending frequency is found in the amplitude spectrum of vertical displacement at mid span. The vertical displacement at mid span is also contributed by the response of first symmetric vertical bending mode with a frequency of 0.1721 Hz.

Table 2 Natural modal frequencies of the catwalk under a design wind speed of 25.7 m/s (Hertz)

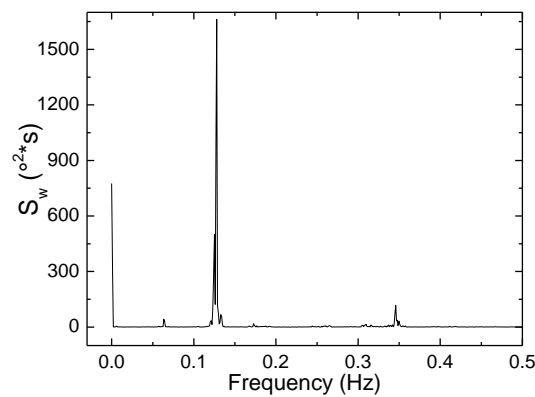| Mode number	Characteristics of mode	Natural frequency
1	1st symmetric lateral bending	0.0633
2	1st anti-symmetric lateral bending	0.1221
3	1st anti-symmetric lateral bending + 1st anti-symmetric vertical bending +1st anti-symmetric torsion	0.1247
4	1st anti-symmetric lateral bending + 1st anti-symmetric vertical bending +1st anti-symmetric torsion	0.1283
5	1st symmetric vertical bending	0.1728
6	1st symmetric torsion	0.1812

Fig. 31 Power spectrum of torsional displacement time-procedures at 3/8 span
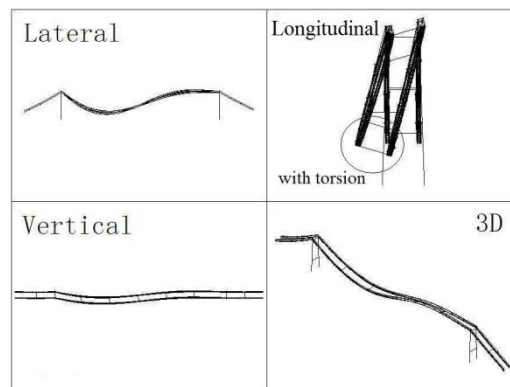

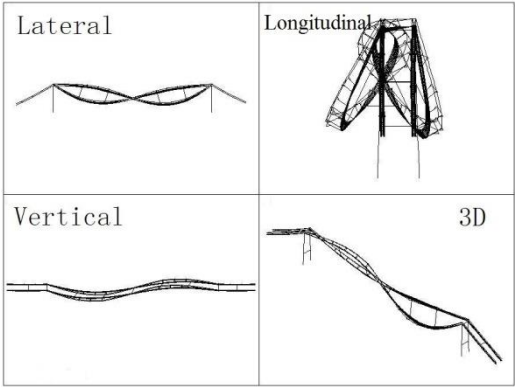Fig. 32 The second modal shape of catwalk under the wind of 25.7 m/s

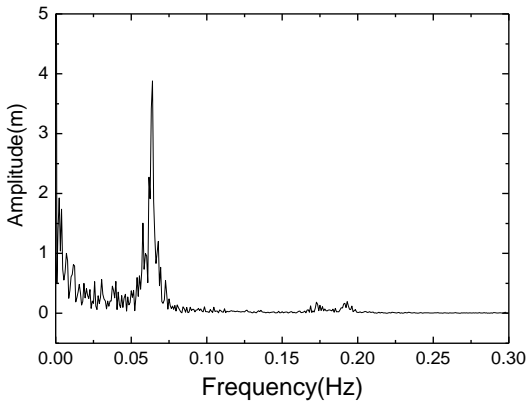Fig. 33 The fourth modal shape of catwalk under the wind of 25.7 m/s

Fig. 34 Amplitude spectrum of lateral displacement at mid span
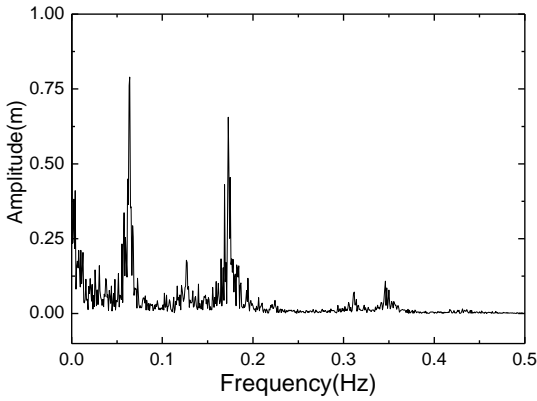

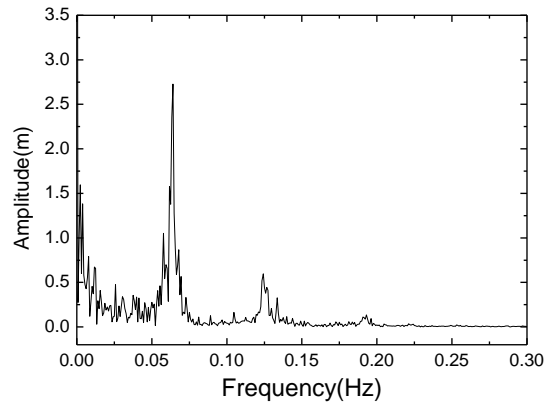Fig. 35 Amplitude spectrum of vertical displacement at mid span

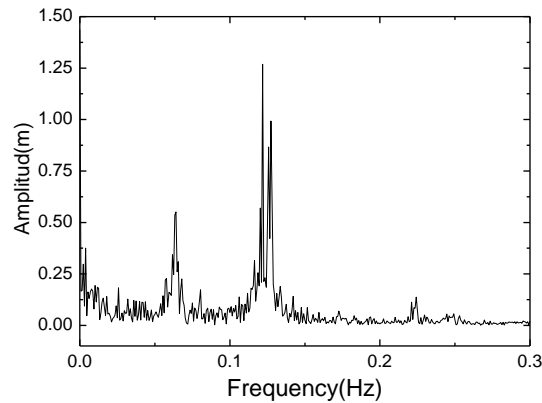Fig. 36 Amplitude spectrum of lateral displacement at 1/4 span

Fig. 37 Amplitude spectrum of vertical displacement at 1/4 span

In the vertical displacement at ¼ span, the first lateral bending frequency is no longer the dominant frequency and the main contribution is 0.1258Hz, which is associated with the third mode. At ¼ span, the main pattern of vibration should be lateral bending, vertical bending, and torsion. In general, the vibration of catwalk is multi-mode, which is due to the characteristics of the cable structure; and the global vibration of catwalk is similar to the fourth modal shape shown in Fig. 33, where the distribution of torsional displacement is anti-symmetric.

5. Conclusions

This paper has presented the aerostatic and the buffeting response analysis of catwalk of a suspension bridge. The three-dimensional static analysis showed the geometric nonlinearity and the nonlinear dependence of wind loading on angle of attack. The results showed strong coupling between lateral and vertical displacements; this is different from the response of a suspension bridge deck. The three-dimensional static displacements increase with increasing wind speed and

the static divergence is not observed. Owing to the existence of the gantries, the torsional displacement is limited in the vicinity of gantry. Local torsional deformation can be effectively controlled. This is an important reason why the catwalk equipped with gantries is widely adopted at the present time.

Under a design wind speed of 25.7 m/s, a time domain analysis of catwalk buffeting response indicates that the lateral displacement is the main pattern of the buffeting response of a catwalk. The lateral displacement is dominated by the first symmetric lateral modal response. This modal response associated with a coupled lateral and vertical motion had a significant contribution to the vertical response at mid span. The vertical displacement was also contributed by the modal responses associated with vertical modal shapes. The torsional displacement is dominated by the modal response associated with coupled vertical and torsional motions.

Acknowledgments

References

Cao, Y.H., Xiang, H.F. and Zhou, Y. (2000), "Simulation of stochastic wind velocity field on long-span bridges", *J. Eng. Mech. - ASCE*, **126**(1), 1-6.

Chen, X. and Kareem, A. (2001), "Nonlinear response analysis of long span bridge under turbulent winds", *J. Wind Eng. Ind. Aerod.*, **89**(14-15), 1335-1350.

Chen, X., Matsumoto, M. and Kareem, A. (2000), "Aerodynamic coupling effects on flutter and buffeting of bridges", *J. Eng. Mech. - ASCE*, **126**(1), 17-26.

Cheng, J., Jiang, J.J., Xiao, R.C., *et al*. (2002), "Nonlinear aerostatic stability analysis of Jiangyin suspension bridge", *Eng. Struct.*, **24**, 773-781.

Davenport, A.G. (1962a), "Buffeting of a suspension bridge by stormy winds", *J. Struct. Div.*, **88**, 233-268.

Davenport, A.G. (1962b), "The response of slender line-like structures to a gusty wind", *ICE Proceedings*, 389-407.

Ding, Q. and Lee, P.K.K. (2000), "Time domain buffeting analysis of suspension bridges subjected to turbulent wind with effective attack angle", *J. Sound Vib.*, **233**(2), 311-327.

Jain, A., Jones, N. and Scanlan, R.H. (1996), "Coupled flutter and buffeting analysis of long-span bridges", *J. Struct. Eng. - ASCE*, **122**(7), 716-725.

Kimura, K. and Tanaka, H. (1992), "Bridge buffeting due to wind with yaw angles", *J. Wind Eng. Ind. Aerod.*, **41-44**, 1309-1320.

Kwon, S.D., Lee, H., Lee, S. and Kim, J. (2012), "Mitigating the effect of wind on suspension bridge catwalks", *J. Bridge Eng.*, **18**(7), 624-632.

Larsen, A. (1997), "Prediction of aeroelastic stability of suspension bridges during erection", *J. Wind Eng. Ind. Aerod.*, **72**, 265-274.

Li, Y.L., Liao, H.L. and Qiang, S.Z. (2004), "Simplifying the simulation of stochastic wind velocity fields for long cable-stayed bridges", *Comput. Struct.*, **82**(20-21), 1591-1598.

Li, Y.L., Ouyang, W., Hao C. and Wang B. (2009), "Study on shape and mechanism of aerostatic stability for long span suspension bridges", *ACTA Aerod. Sinica*, **27**(6), 701-706. (In Chinese)

Li, N., Liu, B., Li J. and Bai, H. (2013), "Analysis of nonlinear aerostatic response for catwalk of Lishui suspension bridge", *J. Architect. Civil Eng.*, **30**(1), 60-65. (In Chinese)

Ministry of Transport of the People's Republic of China. (2004), Wind-resistant Design Specification for Highway Bridges(JTG/T D60-01—2004), China Communications Press, Beijing, China. (In Chinese)

Scanlan, R.H. (1978), "The action of flexible bridges under wind. II: Buffeting theory", *J. Sound Vib.*, **60**(2), 201-211.

Shinichi, H. (1997), "Design and construction of the catwalk for the Kurushima bridges", *Bridge Found. Eng*., **31**(16), 13-19. (In Japanese).

Thai, H.T. and Kim, S.E. (2011), "Nonlinear static and dynamic analysis of cable structures", *Finite Elem. Anal. Des.*, **47**(3), 237-246.

Xu, Y.L. and Sun, D.K. (1998), "Buffeting analysis of long span bridges: a new algorithm", *Comput. Struct.*, **68**(4), 303-313.

Zheng, S.X., Liao, H.L. and Li, Y.L. (2007), "Stability of suspension bridge catwalks under a wind load", *Wind Struct.*, **10**(4), 367-382.

JH